

Wake Fields, Impedance & Collective Effects

Stefano De Santis

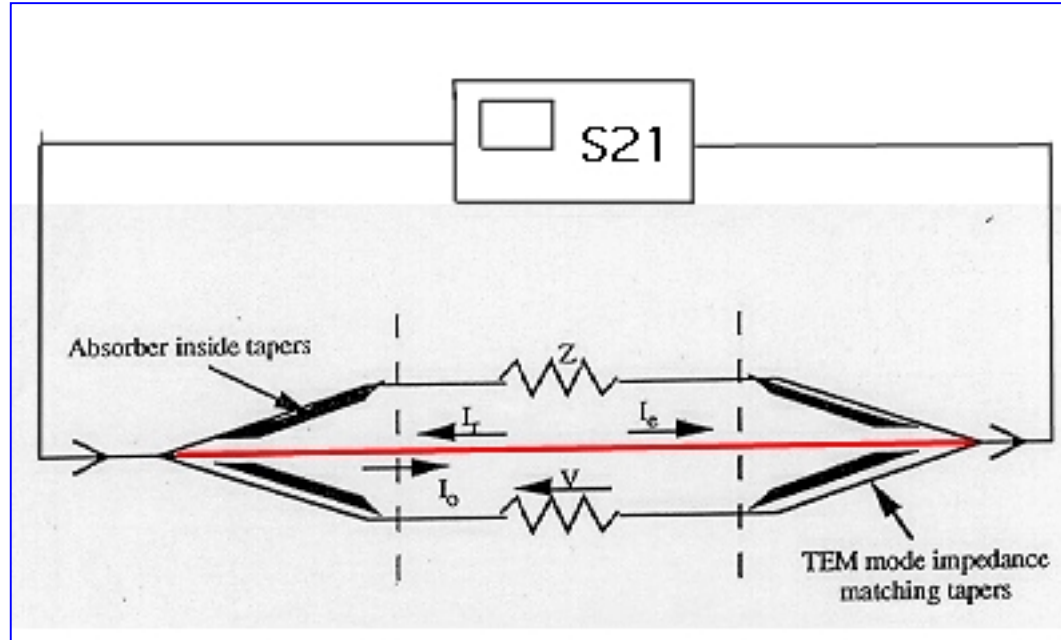
LBNL - CBP

Summary

- Theoretical calculations of wake fields and impedance.
- Bench measurements (RTA, SPEAR3).
- Single-bunch wake fields effects (Femtosource).
- Coupled-bunch instabilities (NLC DRs).

Wake fields (= impedance via Fourier transform), describe the interaction between beam and accelerator.

Coaxial Wire Method



- Critical factors:
- *tapers*
 - *HOMs*
 - *absorbers*
 - *matching network*
 - *wire sagging*
 - *wire diameter*

Measured S_{21} has to be corrected for phase delay and effects of tapers/absorbers. This is usually done remeasuring S_{21} with a reference tube of the same length in place of the component.

Formulas Used in Longitudinal Impedance Measurements

"Short" objects (with respect to λ):

$$\circ Z_{HP} = 2Z_0 \frac{1 - S_{21} / S_{21}^{ref}}{S_{21} / S_{21}^{ref}} \approx Z_{SR} = 2Z_0 \left(1 - S_{21} / S_{21}^{ref} \right) \quad (\text{Hahn - Pedersen and Sands - Rees})$$

"Long" objects:

$$\circ Z_{\log} = -2Z_0 \ln(S_{21} / S_{21}^{ref}) \quad (\text{Walling or log})$$

$$\circ Z_{LOG} = -2Z_0 \ln(S_{21} / S_{21}^{ref}) \left[1 + j \frac{\ln(S_{21} / S_{21}^{ref})}{2kL_i} \right] \quad (\text{Improved log})$$

It can be demonstrated the, in principle, with this method one can exactly measure the impedance of the component under test with the coaxial wire inside.

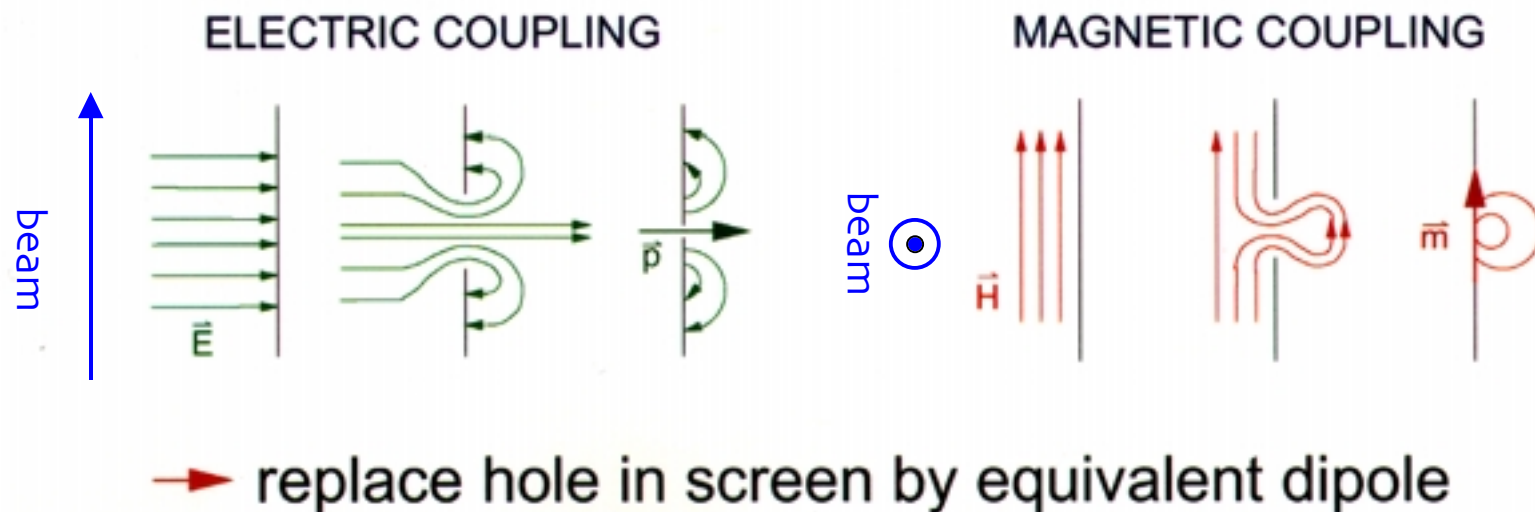
Coaxial Wire Measurements and the Modified Bethe's Diffraction Theory

- To what extent does the coaxial wire perturb the measurement ?
- The Modified BDT (originally developed to calculate impedances theoretically) can help by calculating theoretically the measurement result and comparing it to the theoretical value of the impedance.

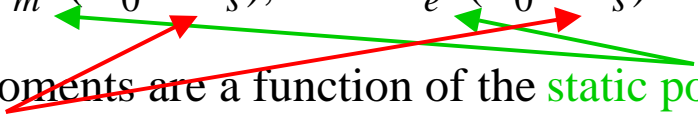
Modified Bethe's Diffraction Theory - A Primer

Analytical model

- Modified Bethe theory for diffraction at small holes was used to study influence of slot parameters




Modified BDT

$$\vec{M} = \vec{\alpha}_m \cdot (\vec{H}_0 + \vec{H}_s), \quad \vec{P} = \epsilon \vec{\alpha}_e \cdot (\vec{E}_0 + \vec{E}_s)$$


The equivalent dipole moments are a function of the static polarizability tensors and of the scattered fields.

$$\vec{E}_s = f(\vec{M}, \vec{P}), \quad \vec{H}_s = g(\vec{M}, \vec{P})$$

The scattered fields are themselves a function of the equivalent dipole moments. This allows to obtain the equivalent dipole moment by solving a linear system:

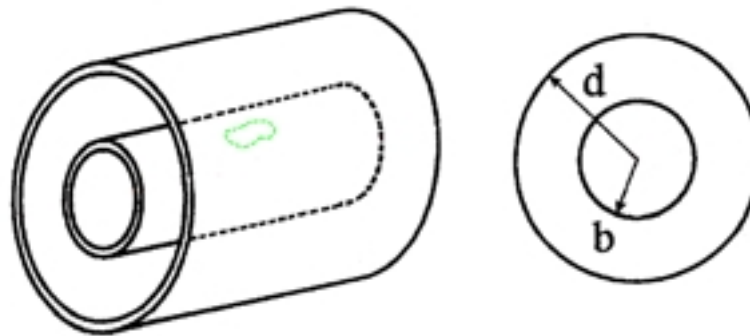
$$[\underline{S}] \begin{bmatrix} \vec{M} \\ \vec{P} \end{bmatrix} = \begin{bmatrix} \vec{\alpha}_m \cdot \vec{H}_0 \\ \epsilon \vec{\alpha}_e \cdot \vec{E}_0 \end{bmatrix}$$


The coefficients matrix **[S]** is a function of the modes chosen to represent the electromagnetic fields. Its expression is particularly simple in the low frequency approximation, when only one propagating mode is used.

The terms outside the principal diagonal represent coupling between apertures.

Modified BDT (cont.)

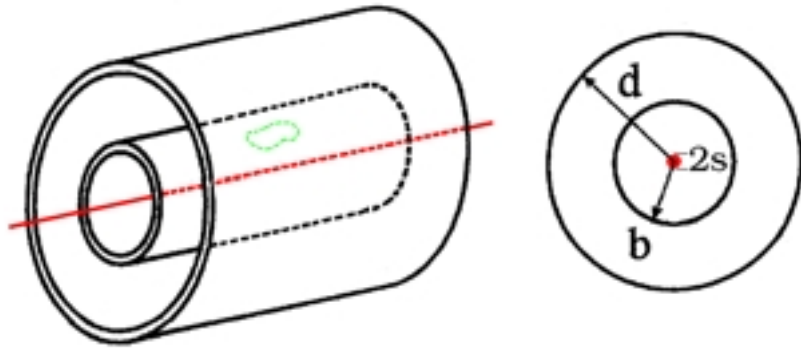
GEOMETRICAL MODEL:



The impedance can be directly calculated using the modified Bethe's diffraction theory:

$$Z_{//} = \frac{k_0 Z_0}{4\pi^2 b^2} \left[j(\alpha_e + \alpha_{m\perp}) + \frac{k_0(\alpha_e^2 + \alpha_{m\perp}^2)}{4\pi b^2 \ln(d/b)} \right]$$

Mod. BDT applied to the experimental set-up



Using BDT we can calculate the S_{21} , as it would be ideally measured, and use this value in the various formulas:

$$Z_{HP} = \frac{k_0 Z_0}{4\pi^2 b^2} \left[j(\alpha_e + \alpha_{m\perp}) + \frac{k_0 \left[(\alpha_e^2 + \alpha_{m\perp}^2) - 2\alpha_e \alpha_{m\perp} \frac{\ln(d/s)}{\ln(b/s)} \right]}{4\pi b^2 \ln(d/b)} \right]$$

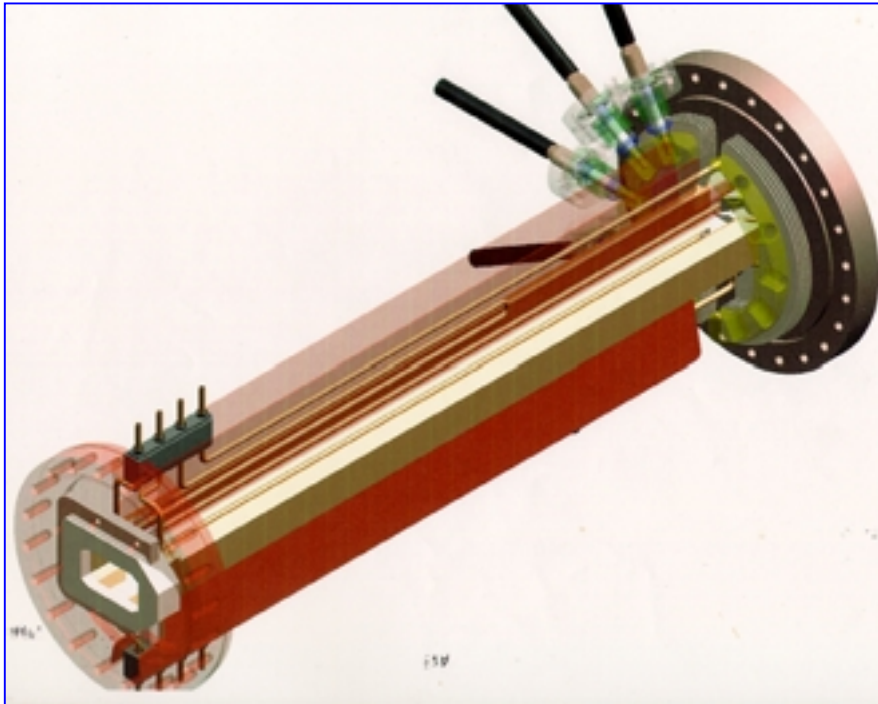
$$Z_{SR} = \frac{k_0 Z_0}{4\pi^2 b^2} \left[j(\alpha_e + \alpha_{m\perp}) + \frac{k_0 \left[(\alpha_e^2 + \alpha_{m\perp}^2) \frac{\ln(d/s)}{\ln(b/s)} \right]}{4\pi b^2 \ln(d/b)} \right]$$

Results (real impedance)

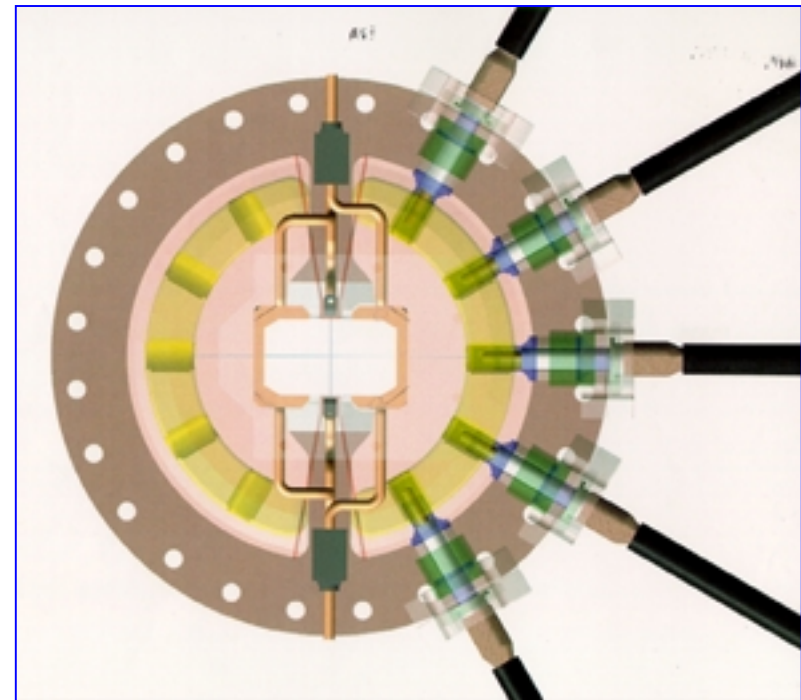
$$Re(Z_{//}) = Re(Z_{SR}) \ln(b/s) / \ln(d/s)$$

- Measured impedance is bigger than the actual one ($d > b$)
- Z_{HP} is always closer to actual value than Z_{SR} .
- But Z_{SR} can be corrected more easily (difference does not depend on α_* 's).
- Same conclusions for distributed impedances. Theoretical value obtained through Differential Modified BDT, compared to Z_{log} . Factor $\ln(d/s)/\ln(b/s)$ is the same.

The SPEAR 3 Injection Kicker



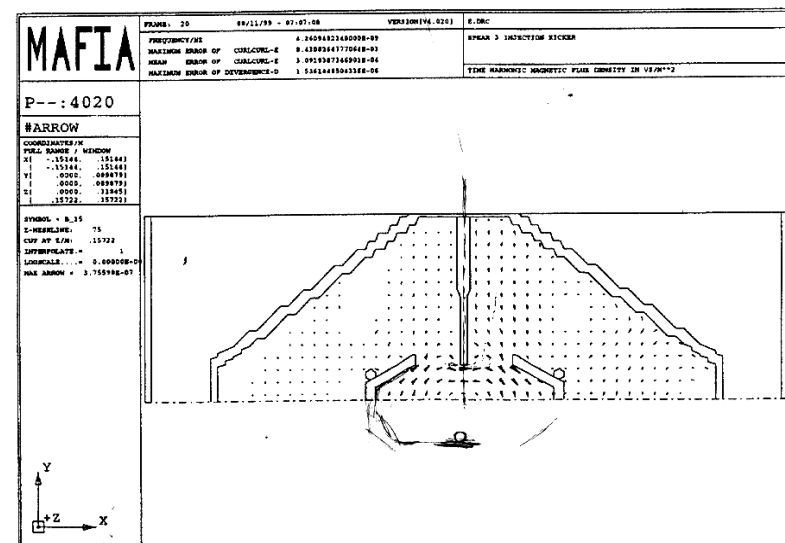
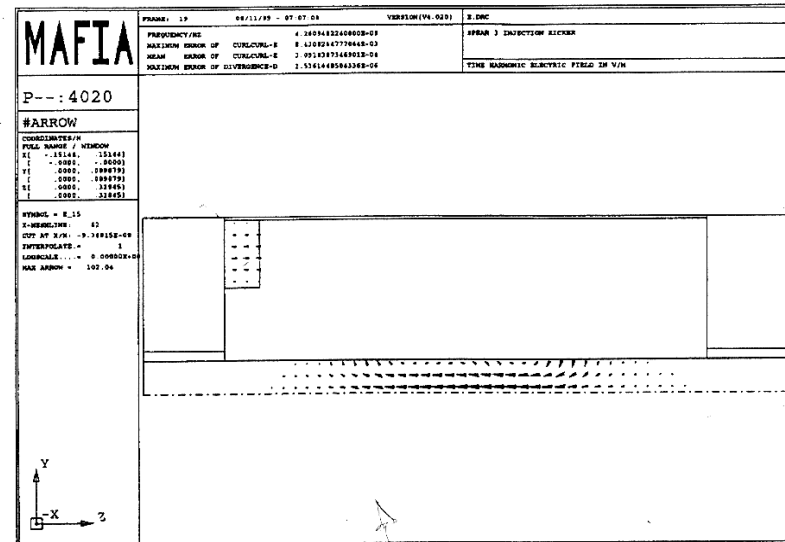
Length: 890 mm



Gap dimensions: 60 x 34 mm
Cut-offs: 2.5 GHz (TE)
5.0 GHz (TM)

High impedance mode at 4.26 GHz (MAFIA).

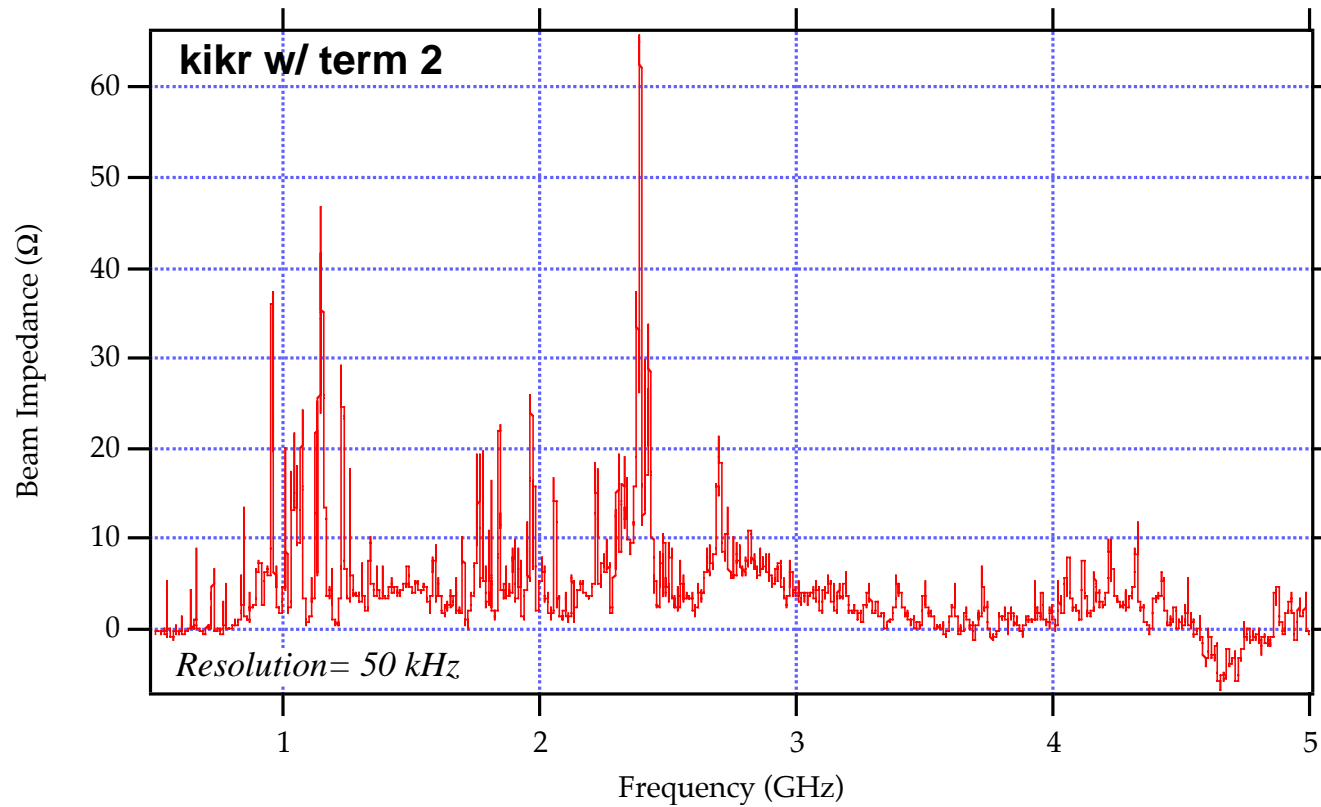
Model run is much shorter than actual kicker, but frequency is dominated by transverse dimensions and should be the same.



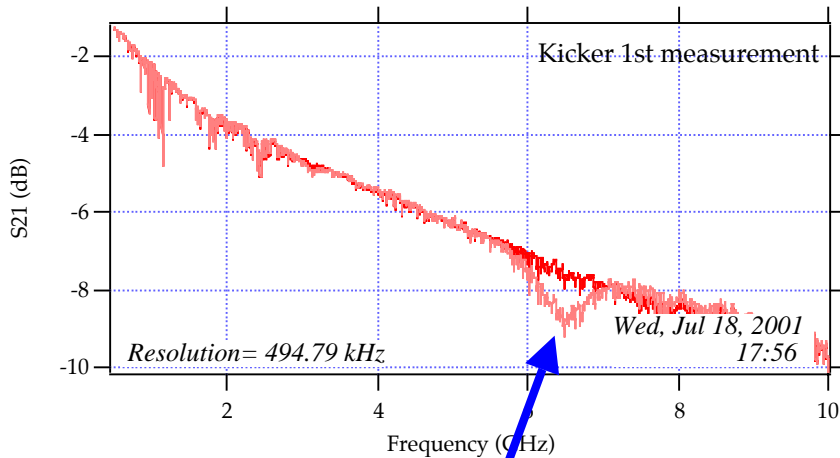
Measurements

- Coaxial Wire.
 - Direct measurement of interaction with beam.
 - Frequencies are shifted.
- Probe Measurements
 - Actual frequencies and Q s measured.
 - Can introduce spurious TEM-like modes.
 - Can't distinguish which resonances couple with beam.
- Perturbation Measurements
 - Can measure R/Q .

Longitudinal Impedance (coax. wire)

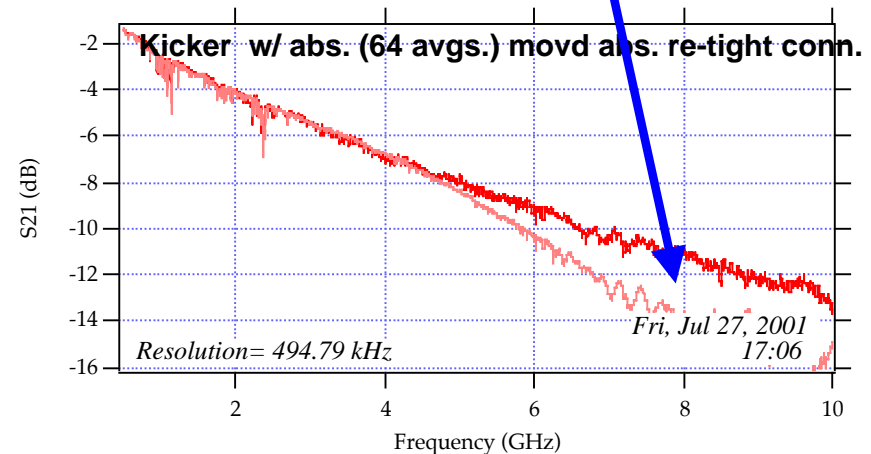


Longitudinal Impedance II: what can go wrong

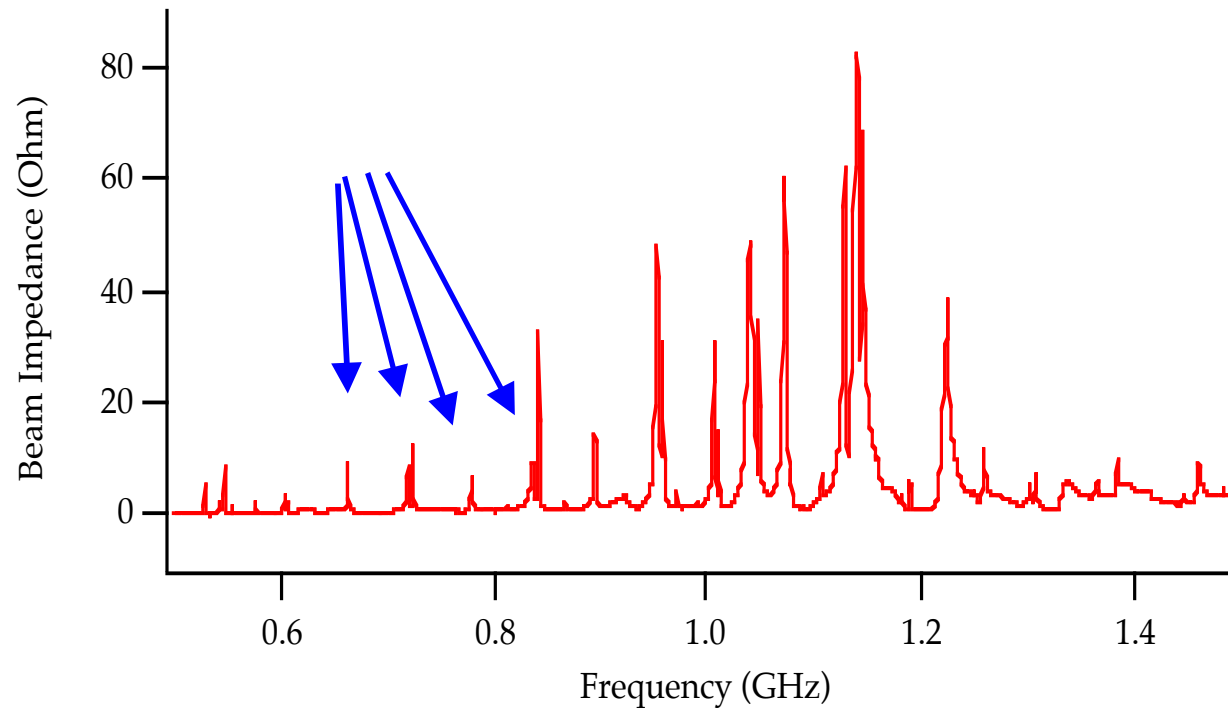


Problem with matching

Not-so-tight connections

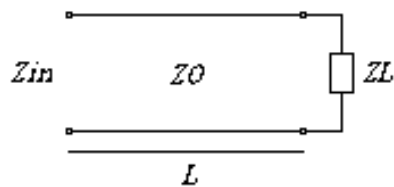


The 60 MHz ripple



60 MHz ripple

Resonances spaced ~ 60 MHz are measured with the stripline connectors open ($Q \approx 2000$). From this measurement it is possible to derive the Q factor of these resonances, when the connectors are terminated using a transmission line model:



$$\begin{aligned} Z_0 &= 80 \, \Omega \\ Z_L &= 0 \text{ (s.c.)} \\ L &= 1.2 \text{ m} \end{aligned}$$

$$\longrightarrow Z_{in} = jZ_0 \tan(2\pi L / \lambda)$$

Reflection coefficient when connectors are terminated on a $13.5 \, \Omega$ line:

$$\Gamma = \frac{Z_{conn} - Z_{in}}{Z_{conn} + Z_{in}} = -0.7$$

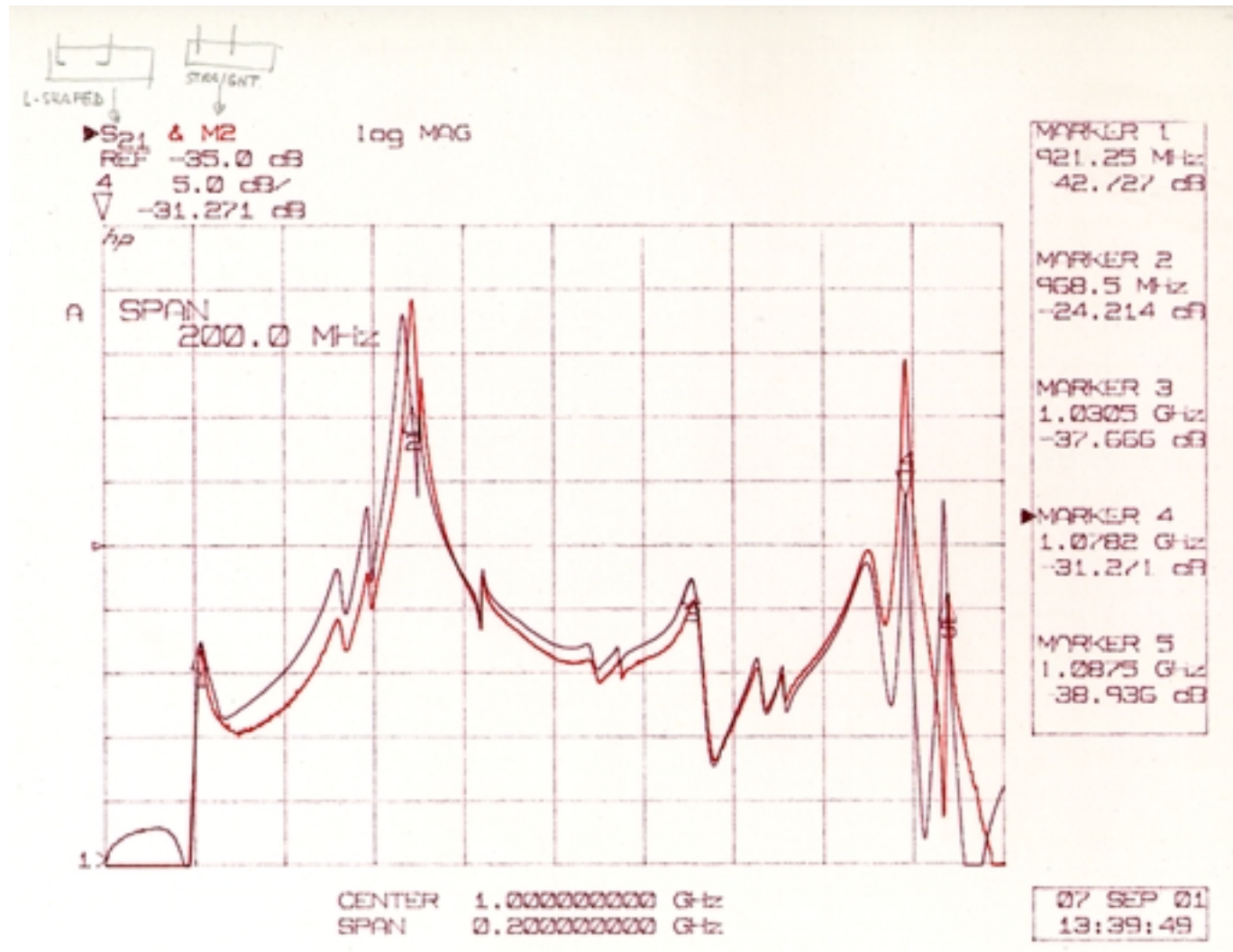


$$Q_{conn} = \frac{2\pi W}{P_l} = \frac{2\pi W(0)/(T/2)}{(1 - \Gamma^2)W(0)/(T/2)} \approx 13$$

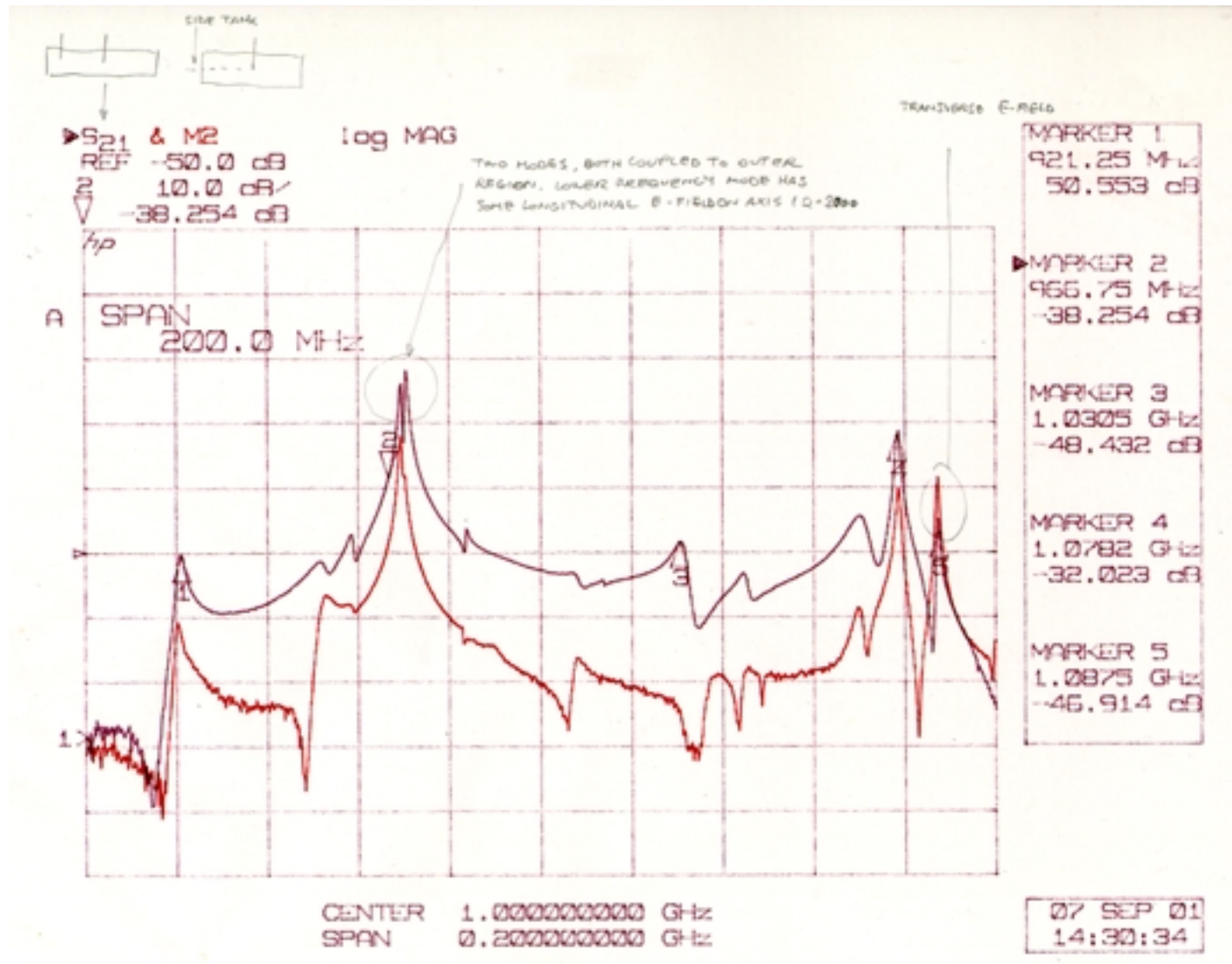
Probe measurements

- Kicker resonances.
 - Different probe shapes (straight, L-shaped, loops) and positions.
- Resonances in outer kicker tank.
 - Probes in outer tank.
- Best position for couplers.
 - Coupling between coaxial wire and probes in outer tank.

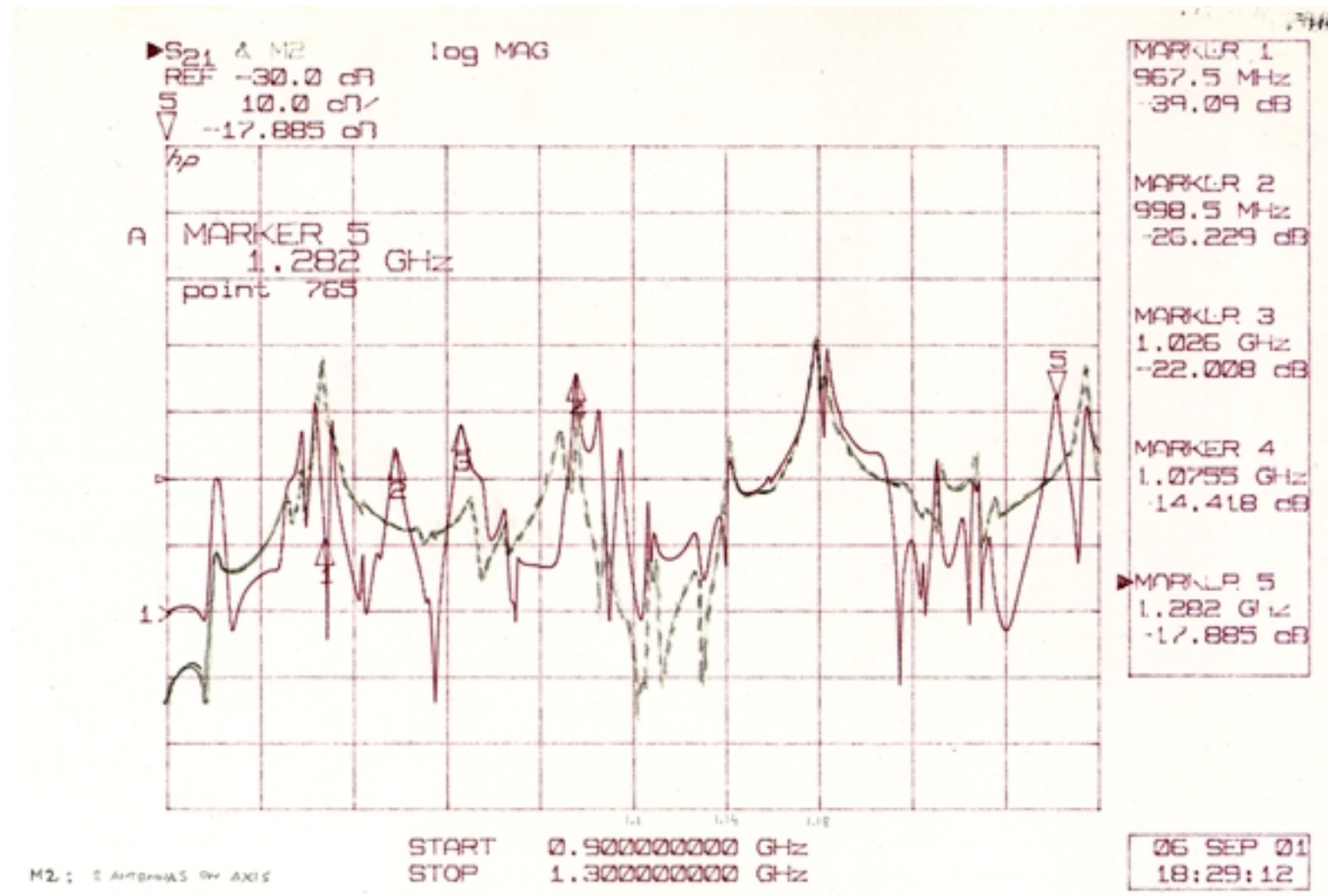
Antennas Measurements I



Antennas Measurements II



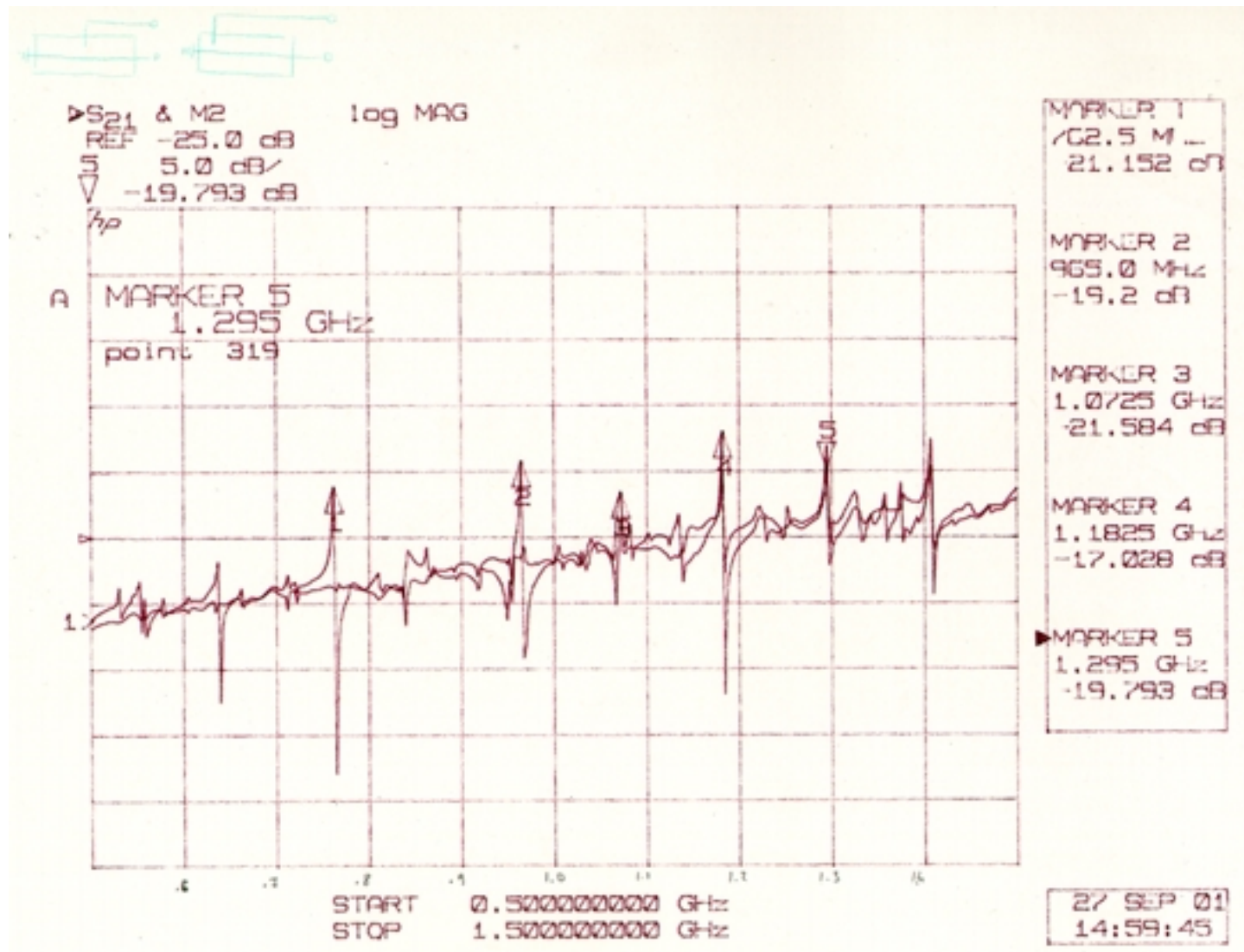
Antennas Measurements III



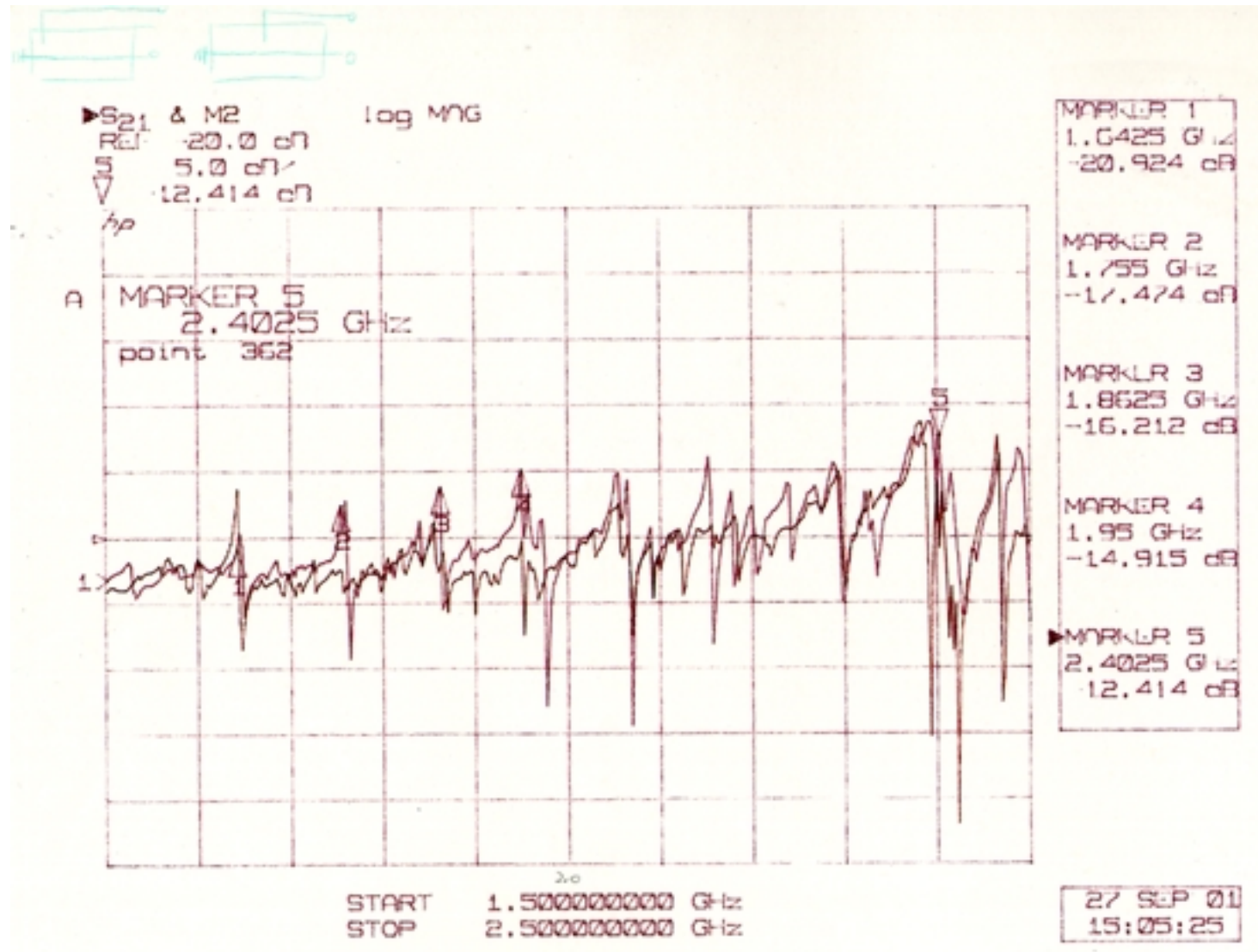
Antennas Measurements Legends

- **I** L-shaped and straight antennas coupling (mostly) to horizontal and vertical E field. The mode at seem to have longitudinal E field on axis.
- **II** The red trace is the coupling to the outer cylinder. Only one of the two peaks at 967 MHz couples out (but this could be due to the particular positions chosen). Also the mode at 1.03 GHz couples weakly outside.
- **III** Shows different antennas positions inside the kicker gap: the continuous trace is obtained with the probes laying on the walls, so that a TEM mode is not supported. In this position though the longitudinal E field is minimum. In the dashed trace the probes were raised up to the kicker axis.

HOM Dampers .5-1.5 GHz



HOM Dampers 1.5-2.5 GHz



Measured Modes

| FREQUENCY [MHz] | Q | FREQUENCY [MHz] | Q |
|-----------------|------|-----------------|------|
| 760 | 600 | 1235 | 1800 |
| 964 | 600 | 1251 | 2100 |
| 1078 | 2400 | 1258 | 1400 |
| 1088 | 2600 | 1302 | 900 |
| 1108 | 3000 | 1380 | 900 |
| 1141 | 700 | 2335 | 5700 |
| 1180 | 400 | 2405 | 1100 |

R/Q Measurements

$$\frac{R}{Q} = \frac{V^2}{2\omega_r W} = \frac{\left(\int \vec{E} \cdot d\vec{z}\right)^2}{2\omega_r W}$$

We can also measure **Q** and, therefore, can calculate **R**

Slater's theorem allows us to measure the integral of the electric field along z:

$$\frac{\Delta f}{f} = \frac{\Delta W_E - \Delta W_H}{W_{TOT}}$$

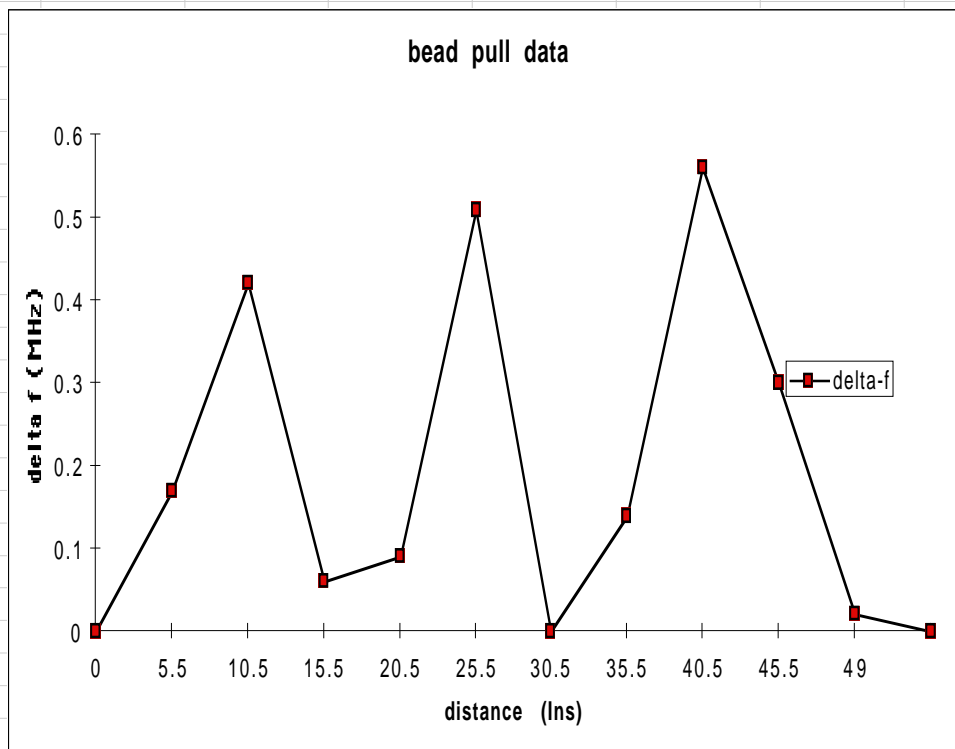
Dielectric sphere:

$$\frac{\Delta f}{f} = -\frac{\pi r^3}{W} \left(\epsilon_0 \frac{\epsilon_r - 1}{\epsilon_r + 2} E_0^2 \right)$$

Metallic needle:

$$\frac{\Delta f}{f} = -\frac{\pi r^2 L}{W} \left(\epsilon_0 E_z^2 - \mu_0 H_z^2 \right)$$

| z (ins) | z (m) | fo (MHz) | fp (MHz) | delta-f | sqrt(delta-f/f) | wz/c | cos(wz/c) | sin(wz/c) | z-parity | sqrt(df/f)cos(wz)sqrt(df/f)sin(wz/c) |
|--------------|--------|----------|----------|---------|-----------------|-------------|-------------|-------------|----------|--------------------------------------|
| 0 | 0 | 2425.5 | 2425.5 | 0 | 0 | 0 | 1 | 0 | 0 | 0 |
| 5.5 | 0.1397 | 2425.5 | 2425.33 | 0.17 | 0.008371896 | 7.096697583 | 0.686950289 | 0.726704411 | 1 | 0.005751076 0.006083894 |
| 10.5 | 0.2667 | 2425.5 | 2425.08 | 0.42 | 0.013159034 | 13.54824084 | 0.555468355 | 0.831537676 | 1 | 0.007309427 0.010942232 |
| 15.5 | 0.3937 | 2425.5 | 2425.44 | 0.06 | 0.004973647 | 19.9997841 | 0.408279159 | 0.912857124 | 1 | 0.002030637 0.004540229 |
| 20.5 | 0.5207 | 2425.5 | 2425.41 | 0.09 | 0.006091449 | 26.45132736 | 0.249544843 | 0.968363243 | 1 | 0.00152009 0.005898735 |
| 25.5 | 0.6477 | 2425.5 | 2424.99 | 0.51 | 0.014500549 | 32.90287061 | 0.08375402 | 0.99648646 | 1 | 0.001214479 0.014449601 |
| 30.5 | 0.7747 | 2425.5 | 2425.5 | 0 | 0 | 39.35441387 | -0.08440516 | 0.996431518 | 1 | 0 0 |
| 35.5 | 0.9017 | 2425.5 | 2425.36 | 0.14 | 0.007597372 | 45.80595713 | -0.25017757 | 0.968199971 | 1 | -0.00190069 0.007355775 |
| 40.5 | 1.0287 | 2425.5 | 2424.94 | 0.56 | 0.015194744 | 52.25750039 | -0.40887558 | 0.912590138 | 1 | -0.00621276 0.013866573 |
| 45.5 | 1.1557 | 2425.5 | 2425.2 | 0.3 | 0.011121413 | 58.70904364 | -0.55601161 | 0.831174527 | 1 | -0.00618363 0.009243836 |
| 49 | 1.2446 | 2425.5 | 2425.48 | 0.02 | 0.002871537 | 63.22512392 | 0.923660575 | 0.383211616 | 1 | 0.002652325 0.001100406 |
| | 0 | 2425.5 | 2425.5 | 0 | 0 | 0 | 1 | 0 | 0 | 0 |
| reversal at> | 0 | | | | | | | | | |
| | | | | | | | | | | 0.006180947 0.073481282 sum |
| | | | | | | | | | | 7.8498E-05 0.000933212 sum * delta-z |
| epsilon= | 9.3 | | RTT/Q= | 5.50 | | | | | | 6.16194E-09 8.70885E-07 (sum*dz)^2 |
| | | | | | | | | | | 8.77047E-07 cos^2 + sin^2 ter |



Excel spreadsheet used for the
R/Q calculations (courtesy of R. Rimmer)

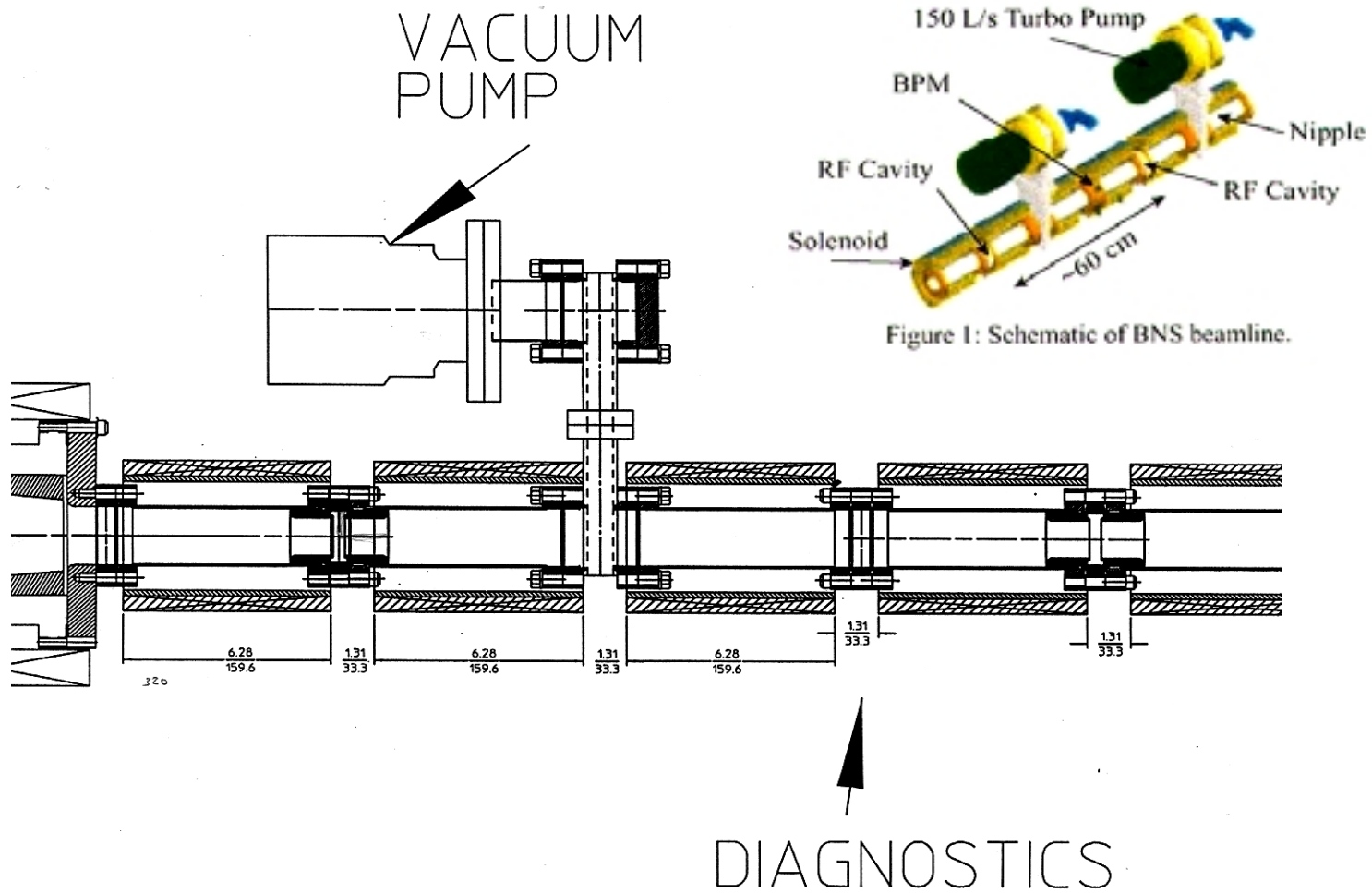
Conclusions

- Mode at 4.26 GHz not observed.
 - Perhaps worth to check MAFIA w/ different length.
- Other modes below 2 GHz seem “external”.
 - Measure of E_z not definitive, but R/Q below noise level.
- Mode at 2.4 GHz has low impedance.
- Best position for damper depends on mode.

Betatron Node Scheme Experiment

- Exciting and measuring BBU growth and its dependance on the betatron tune.
- Measuring the BPM response (transfer impedance) .
- Measuring pillbox cavities frequencies.

BNS Beamline



BNS Pillbox Cavity and BPM Details

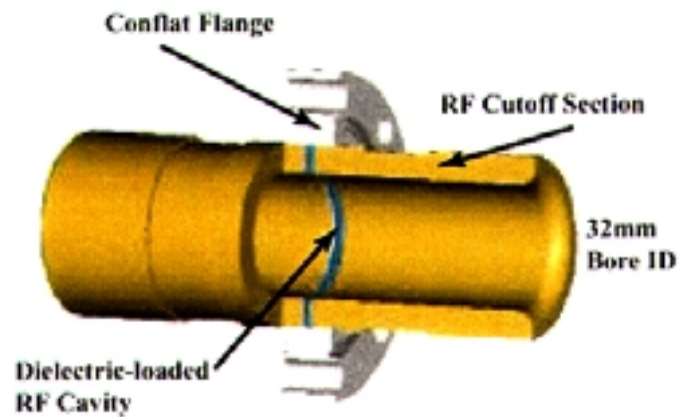


Figure 2: Schematic of dipole-mode pillbox cavity.

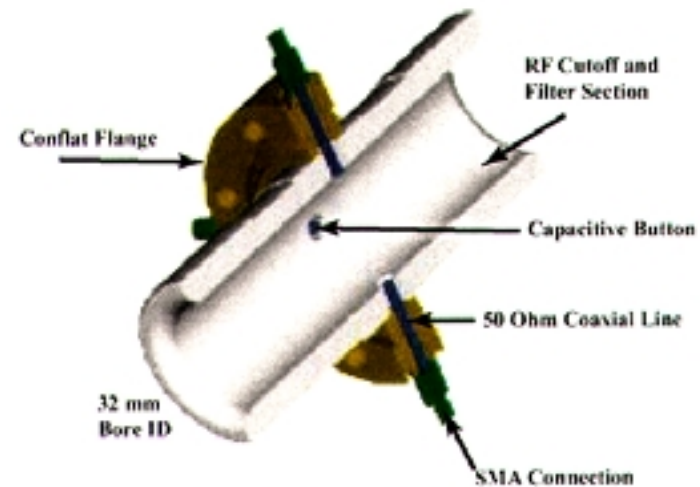
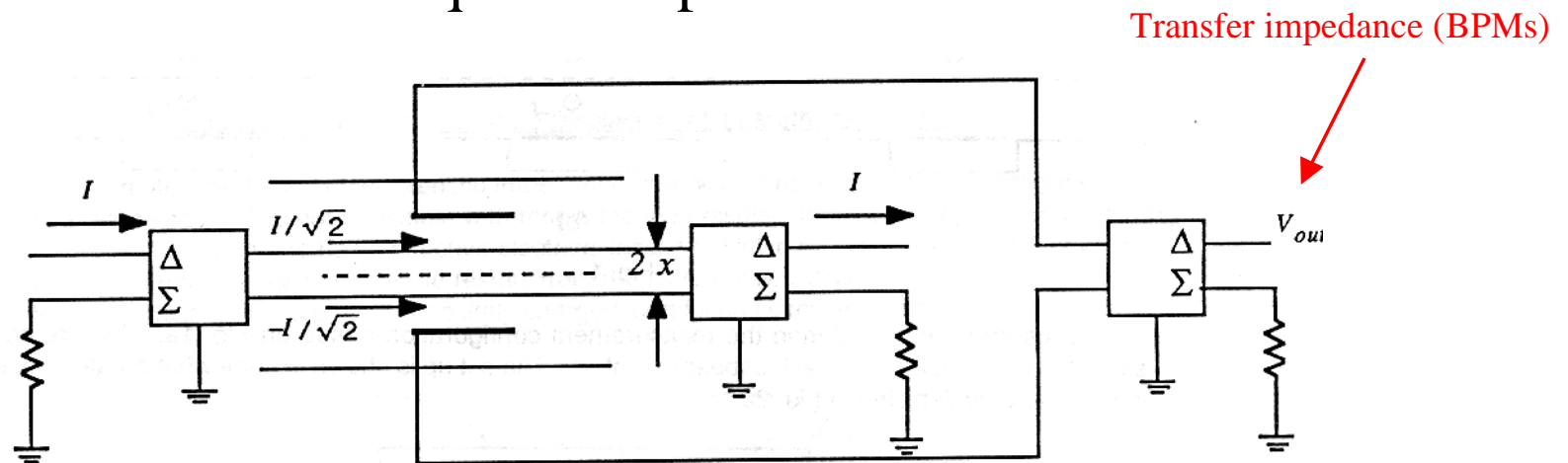


Figure 3: Schematic of capacitive BPM.

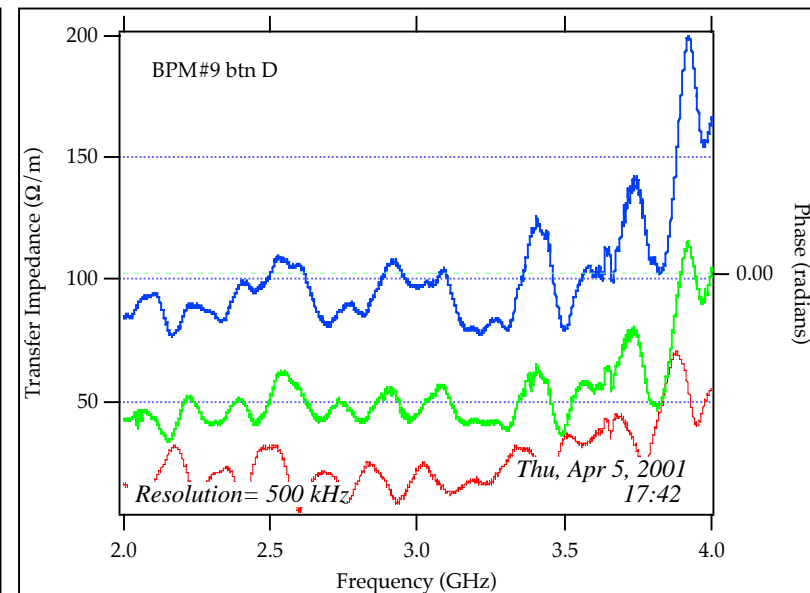
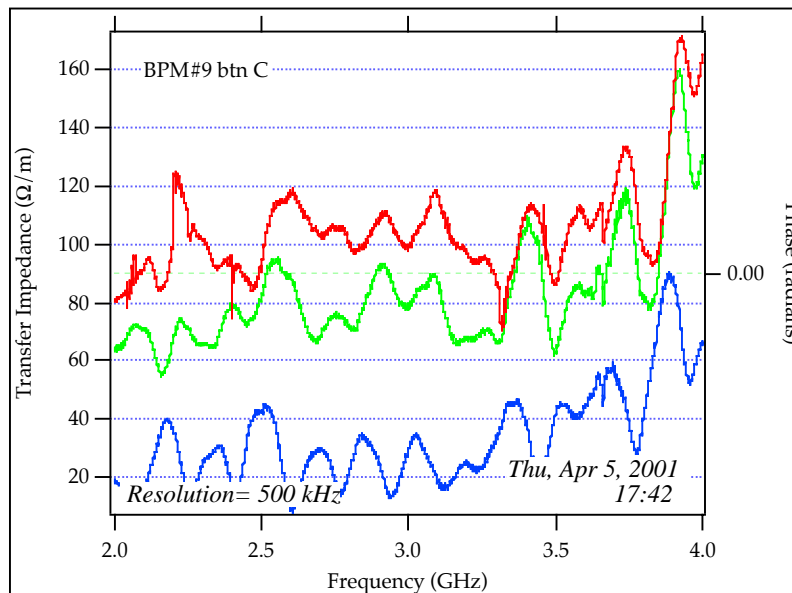
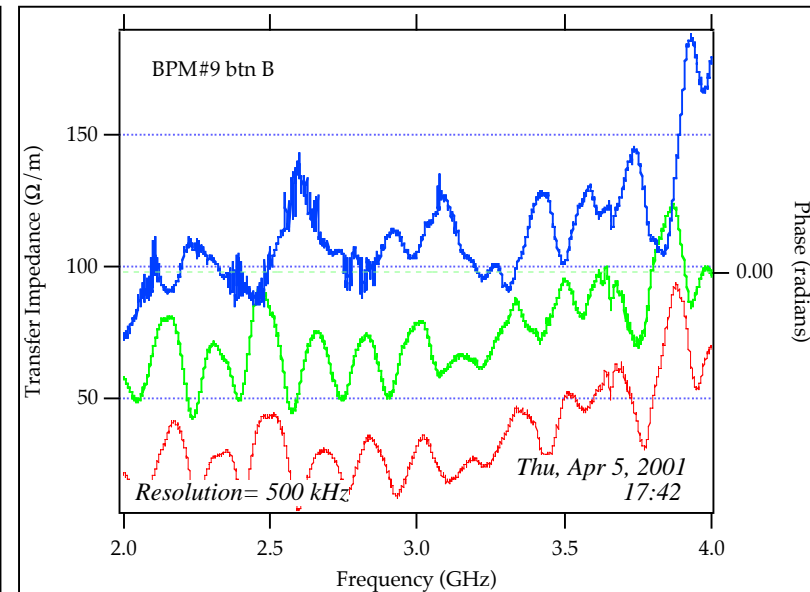
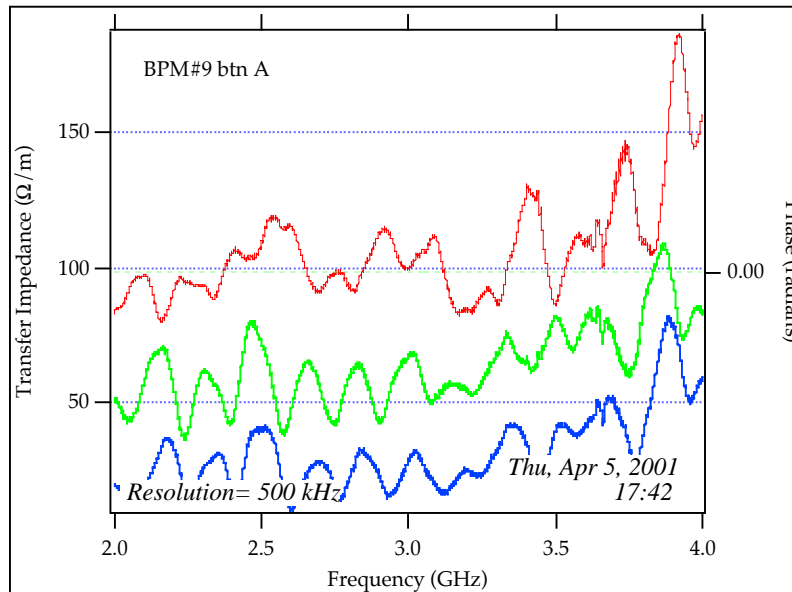
Experimental Set-up

“Coaxial” wire technique for dipole modes



In this case matching is provided by hybrids, provided the two-wire line is $100\ \Omega$ (wire separation)

BPM Transfer impedance



Cavities resonances

Table 1: Pillbox Cavity Dipole Mode Parameters

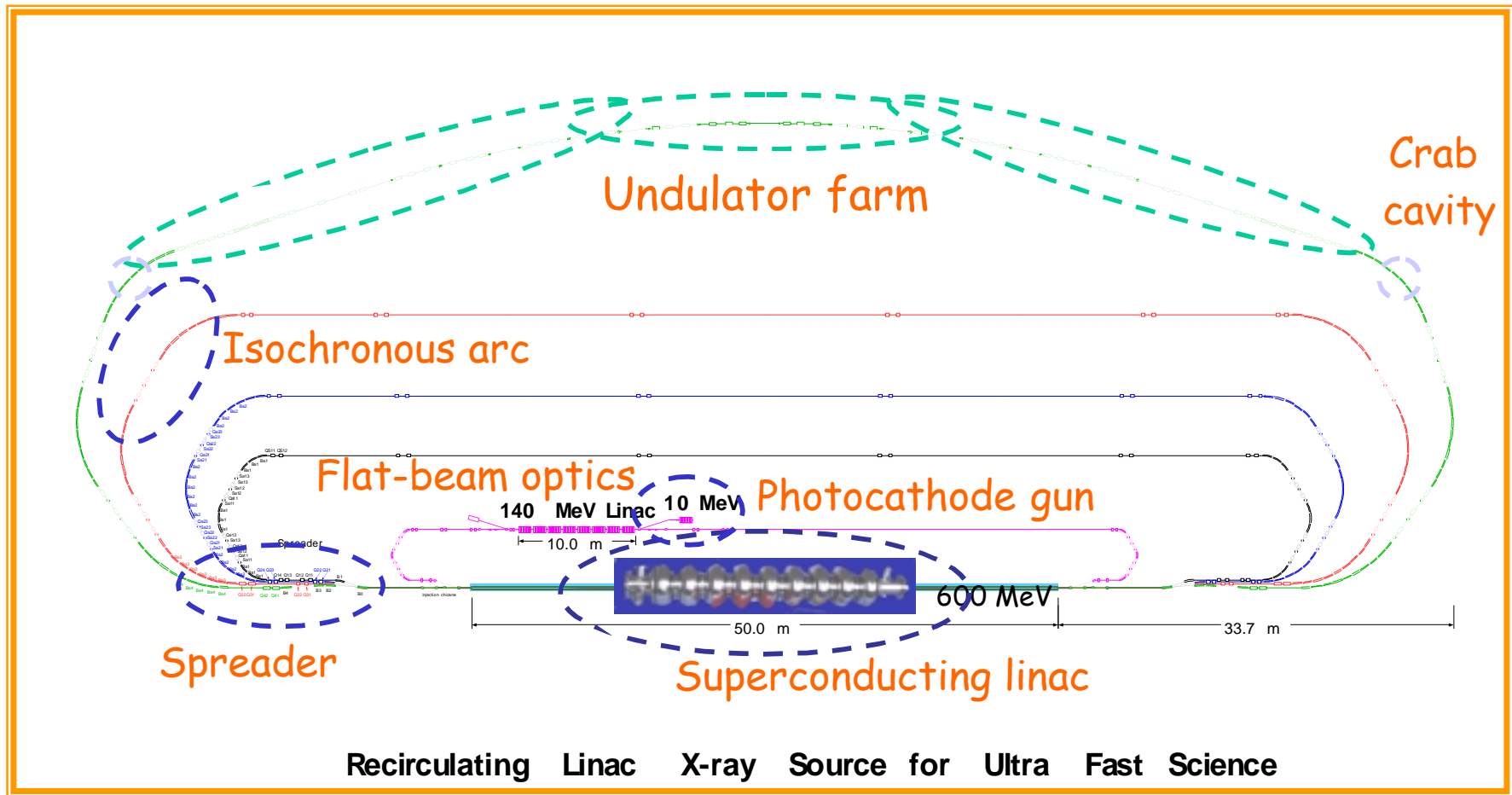
| Cavity | Frequency (GHz) | Q |
|--------|-----------------|-----|
| 1 | 3.76 | 100 |
| 2 | 3.794 | 120 |
| 3 | 3.754 | 110 |
| 4 | 3.925 | 140 |
| 5 | 3.85 | 110 |
| 6 | 3.99 | 120 |
| 7 | 3.715 | 130 |
| 8 | 3.377 | 150 |
| 9 | 3.5 | 100 |

The dielectric in some cavities was changed to reduce the spread in the dipole frequencies.

Berkeley Femtosource

- Study of beam break-up (BBU) instability and possible cures.
- Effects of linac misalignments, injection jitter, short- and long-range wakefields were taken into account.
- Femtosource linac has no focussing elements -> analytical solution is possible.

A schematic of the machine



SC 600 MeV Linac

| | |
|-------------------------|--------------------|
| E_{acc} | 20 MV/m |
| Frequency | 1.3 GHz |
| Operation mode | CW |
| Quality factor | 1×10^{10} |
| RF power loss/cavity | 42 W |
| Cavity length | 1.038 m |
| Module length | 12 m |
| Cavities/module | 8 |
| Beam current | 0.04 mA |
| Beam power/cavity | 800 W |
| Q_{beam} | 6×10^8 |
| Bandwidth | 200 Hz |
| Q_{external} | 6.5×10^6 |
| RF power/4 modules | 540 kW |
| RF power loss/4 modules | 1.3 kW |

9-cell superconducting cavity for
TESLA: gradient $E_{\text{acc}} = 23 \text{ MV/m}$

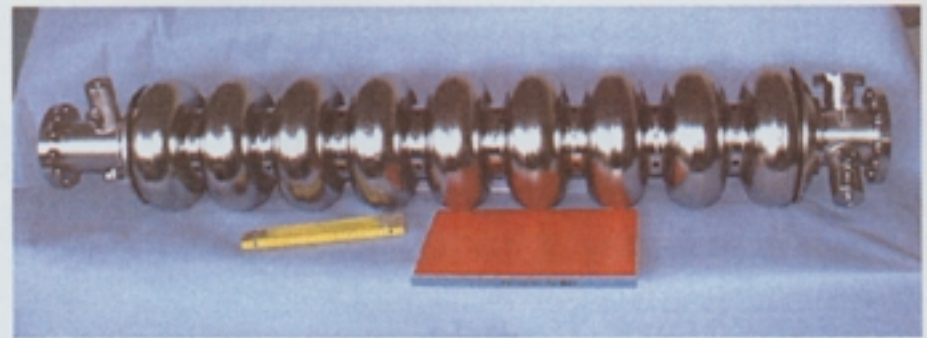
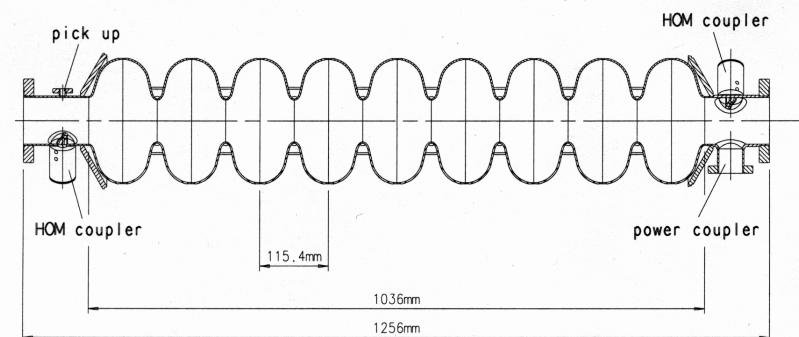


Figure 1.1.1: The 9-cell niobium cavity for TESLA.

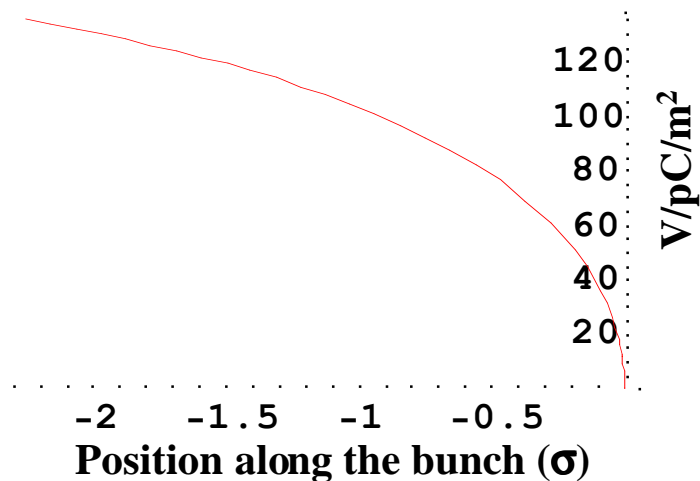


Single-bunch BBU 1

Source: short range wake fields (transverse).

Effect: vertical emittance increase through variable displacement along the bunch.

Transverse wake field for the RF cavities (*from A. Mosnier*):



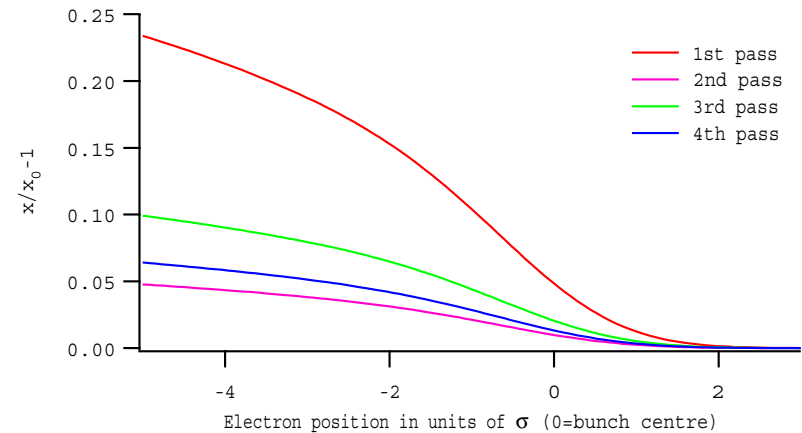
Analytic fit:

$$1290 \sqrt{s} - 2600 s \text{ (V/pC/m}^2\text{)}$$

Single-bunch BBU 2

Since there are no focussing elements in the linac, the equation of motion can be solved by successive iterations:

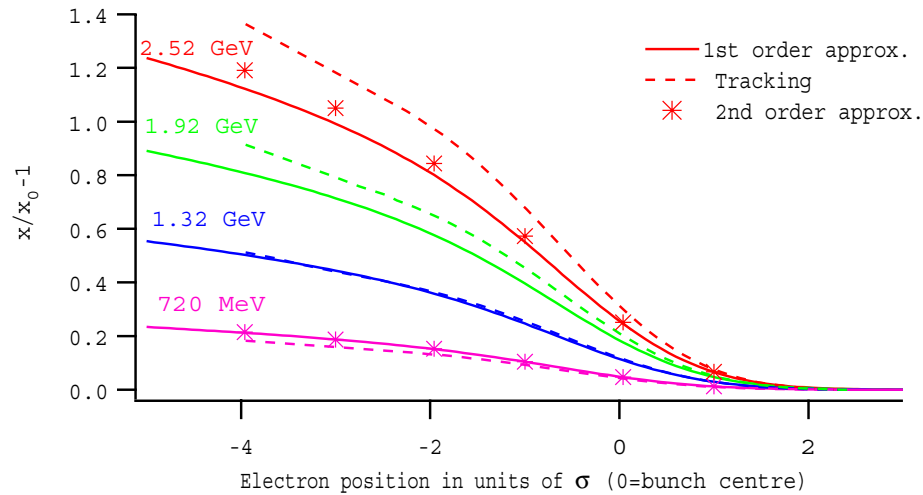
$$\frac{d}{ds} \left[\gamma(s) \frac{d}{ds} y_{(n)}(z, s) \right] = r_0 \int_0^\infty \rho(z - z') W_\perp(z') y_{(n-1)}(z - z', s) dz'$$



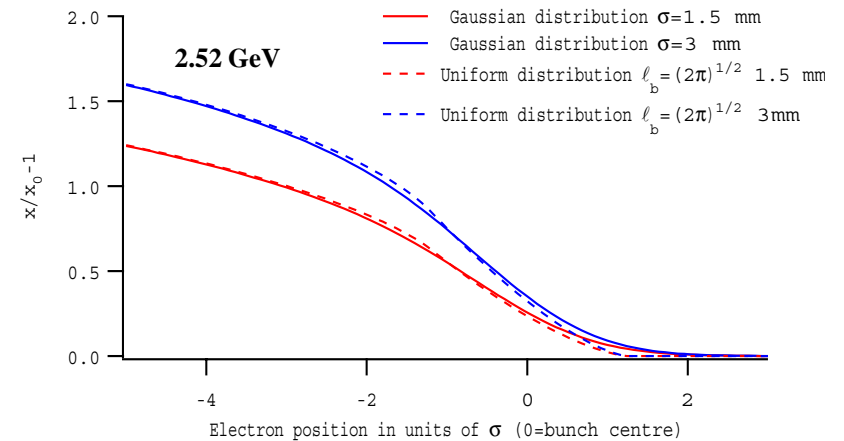
$$y_{(1)}(z, s = L) = y_0 + y_0 \frac{r_0 \gamma_i L^2}{(\Delta \gamma)^2} \int_0^\infty \rho(z - z') W_\perp(z') dz' \left[\frac{\Delta \gamma}{\gamma_i} - \ln \left(1 + \frac{\Delta \gamma}{\gamma_i} \right) \right] + y_0' L \frac{\gamma_i}{\Delta \gamma} \ln \left(1 + \frac{\Delta \gamma}{\gamma_i} \right)$$

Given our machine parameters, the first order solution is already good enough.

Single-bunch BBU 3



The analytical results have been compared to a tracking code output. In the figure above, we assume no initial angle error.



The bunch distribution has a negligible effect on the displacement, which is strongly affected by the bunch length instead.

Main Linac Alignment

Main linac has 32 RF cavities divided in 4 cryomodules.

- Misalignments in RF Cavities: 500 μm rms value (from manufacturer, we can't change it).
- Misalignments in cryomodules: 150 μm rms value (estimate from ALS data).

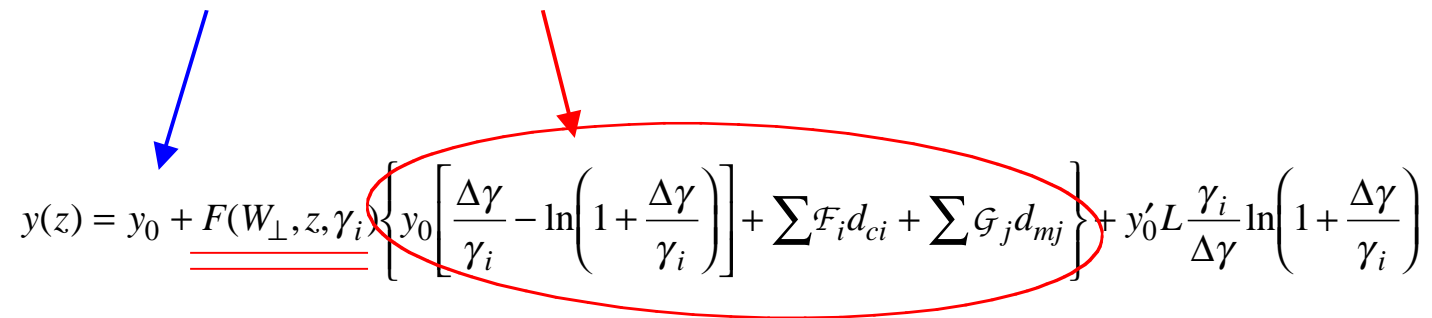
$$\langle y^2 \rangle^{1/2} = \frac{r_0 \gamma_i L^2}{(\Delta\gamma)^2} \int_0^\infty \rho(z - z') W_\perp(z') dz' \sqrt{\sum_{i=0}^{N_{cav}-1} \mathcal{F}_i^2(s) \langle d_c^2 \rangle + \sum_{i=0}^{N_{mod}-1} \mathcal{G}_i^2(s) \langle d_m^2 \rangle}$$

Displacement with no initial error ($y_0 = y'_0 = 0$).

For example, after the first pass, at the bunch centre: $\langle y^2(z=0) \rangle^{1/2} \approx 0.017 \sqrt{1.21 \langle d_c^2 \rangle + 9.30 \langle d_m^2 \rangle}$

Main Linac Alignment: Cures 1

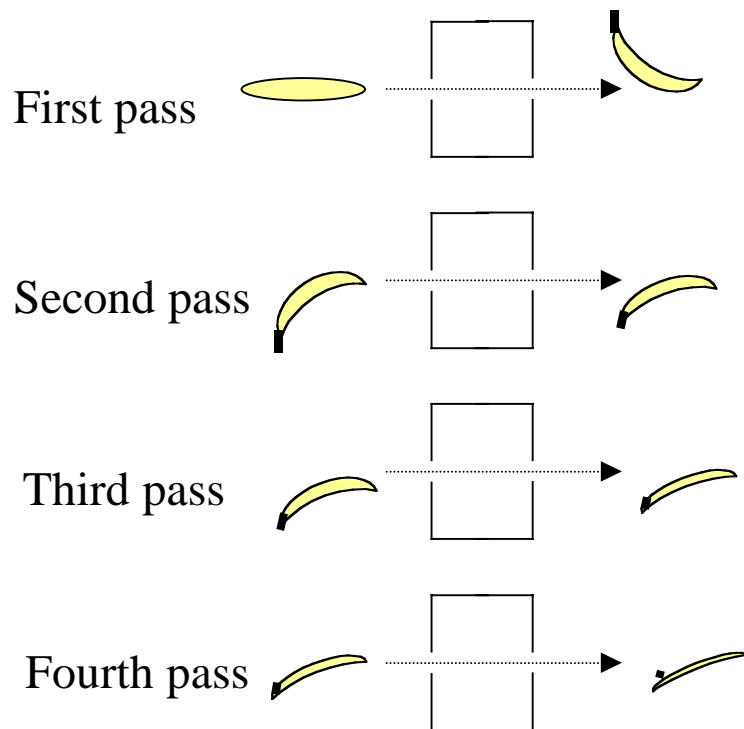
offset increases....tilt is canceled



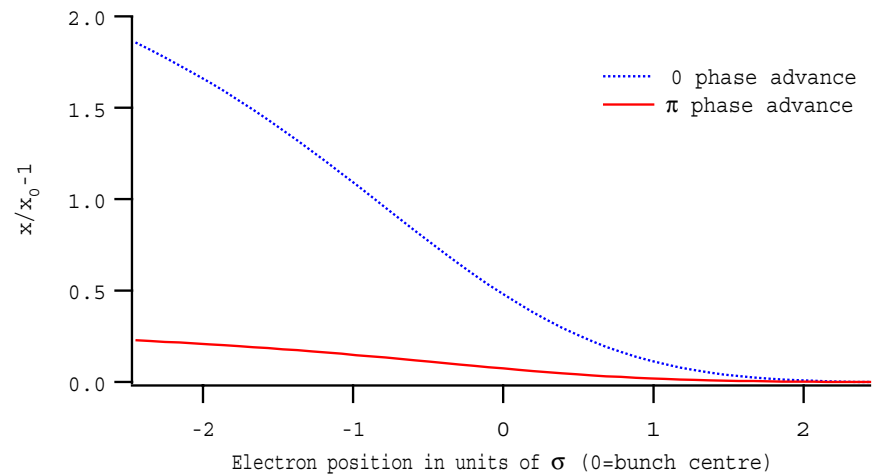
$$y(z) = y_0 + \underline{\underline{F(W_{\perp}, z, \gamma_i)}} \left\{ y_0 \left[\frac{\Delta\gamma}{\gamma_i} - \ln \left(1 + \frac{\Delta\gamma}{\gamma_i} \right) \right] + \sum \mathcal{F}_i d_{ci} + \sum \mathcal{G}_j d_{mj} \right\} + y'_0 L \frac{\gamma_i}{\Delta\gamma} \ln \left(1 + \frac{\Delta\gamma}{\gamma_i} \right)$$

It is possible to cancel the displacement dependence on the particle position inside the bunch (no tilt) by introducing an appropriate initial offset. This requires **accurate BBU measurement**.

Main Linac Alignment: Cures 2



If the **first arc has a phase advance of π** , subsequent passes through the linac tend to cancel the effect of the first pass (there is no total cancellation because of the different energies).



NLC DR Coupled-bunch Instabilities

- Growth rates calculated for:
 - MDR and PDR.
 - Longitudinal and transverse (w/ res. wall).
 - 1.4 and 2.8 ns bunch spacing.
- How to study uneven fills.

Fundamental Parameters

MDR

PDR

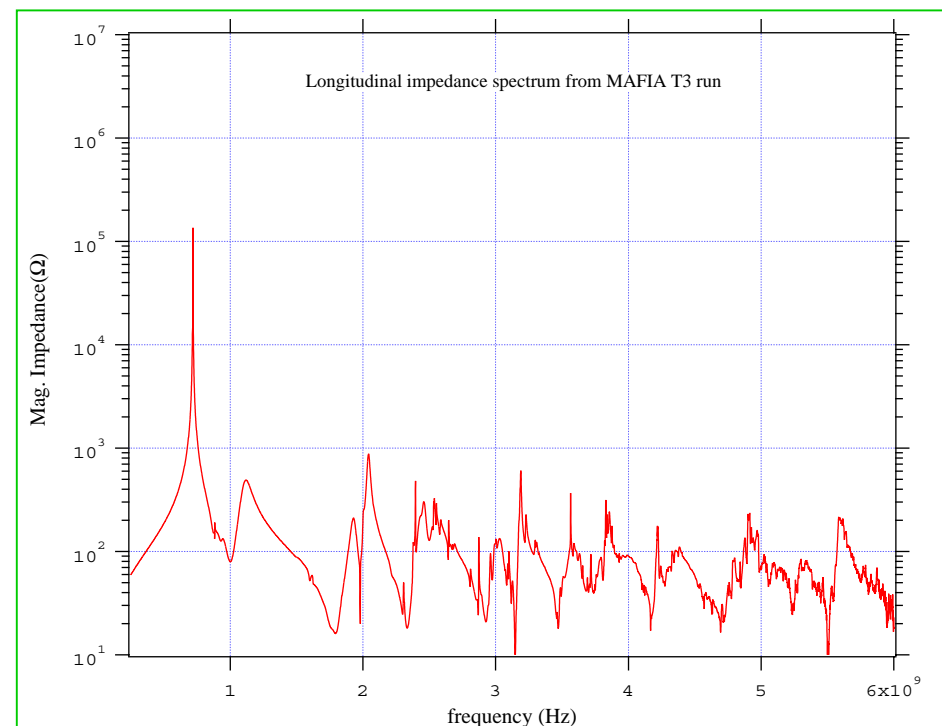
| | | |
|--|-------------------|-------------------|
| Circumference | 299.792 m | 230.933 m |
| Beap pipe radius | 16 mm | 32 mm |
| Wiggler total length | 46.238 m | 49.5 m |
| Wiggler half-gap | 8 mm | 20 mm |
| Energy (E_0) | 1.98 GeV | 1.98 GeV |
| Current (I_0) | 729 mA | 632 mA |
| Bunch length (σ_z) | 12 ps | 17 ps |
| Bunches per train (N_b , fill A/fill B) | 190/95 | 190 |
| Bunch spacing (fill A/fill B) | 1.4/2.8 ns | 1.4 ns |
| Bunch trains stored | 3 | 2 |
| Betatron tune (horiz./vert.) | 27.2616/11.1357 | 11.465/5.388 |
| Synchrotron tune (Q_s) | 0.003496 | 0.0114 |
| Momentum compaction (α) | 0.000295 | 0.002 |
| Damping times (horiz./vert./long.) | 4.85/5.09/2.61 ms | 5.85/5.81/2.89 ms |
| RF voltage | 1.07 MV | 1.516 MV |
| RF frequency (f_{RF}) | 714 MHz | 714 MHz |
| Number of RF cavities | 3 | 4 |
| Total energy loss/turn | 777 keV | 525 keV |
| β at RF cavities location (horiz. and vert.) | 6 m | 6 m |

Harmonic number (h)

714

550

Longitudinal HOMs



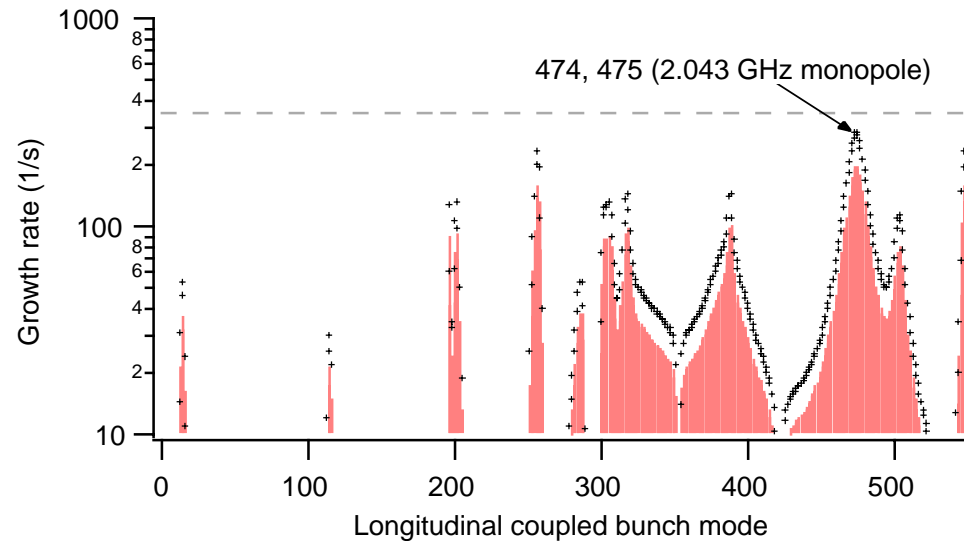
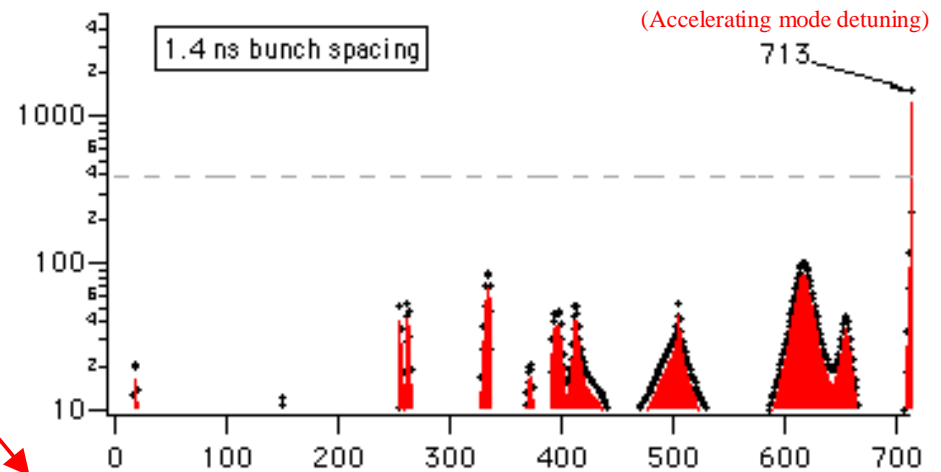
...and Fundamental Formulas

Growth rates, for an even fill:

$$\tau = \left(\frac{I_{tot} \alpha f_{RF}}{2E_0 Q_S} \text{Re}(Z_{//}^{eff}) \right)^{-1}$$

MDR

PDR

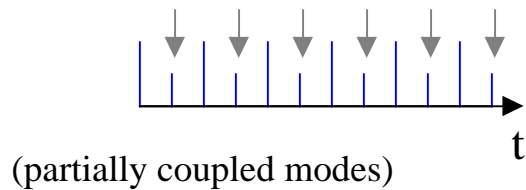
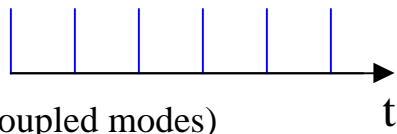
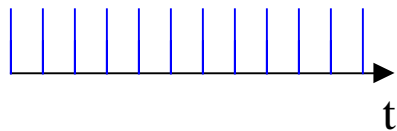


$$f_p(n) = n f_{RF} + p f_{rev} + f_s$$

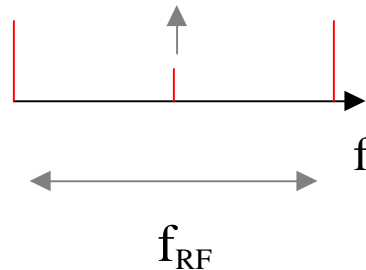
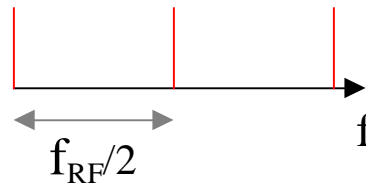
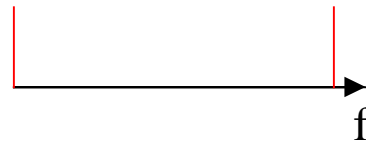
$$Z_{//}^{eff}(p) = \sum_{n=-\infty}^{\infty} \text{sign}(f_p) \frac{f_p}{f_{RF}} \text{Exp}[-(2\pi f_p \sigma_t)^2] Z_{//}(f_p)$$

Basics of Mode Coupling

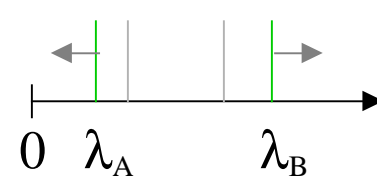
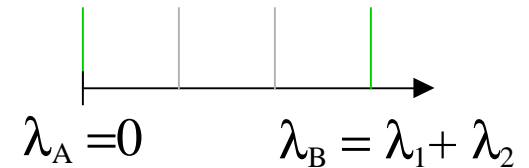
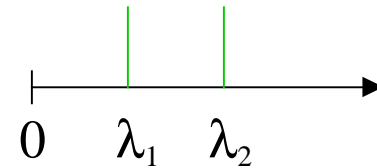
Fill function



Fill spectrum



Eigenvalues



(linear combination of λ_1 and $\lambda_2 < \lambda_1 + \lambda_2$)

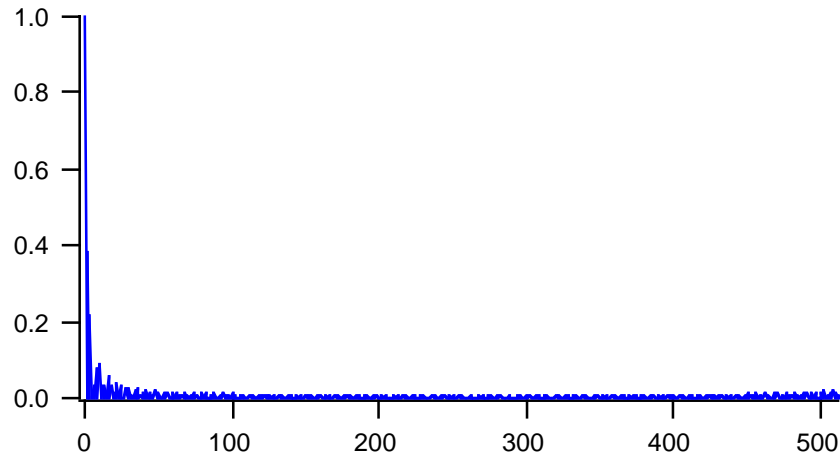
A theorem about fractional fills

- If a uniform fill is stable, adding one gap cannot make it unstable.
- This is still valid for (few) more gaps unless the impedance function is pathological.



Instead of solving the $h \times h$ system, we can just make some considerations on “equivalent” fills, since we are interested in stability and not in the exact growth rates.

PDR and MDR fill spectra



With two bunch trains , the PDR spectrum is quite close to the ideal, uncoupled spectrum. The MDR spectrum is also very similar.

